frontiers | Frontiers in Marine Science

TYPE Original Research
PUBLISHED 09 February 2023
DOI 10.3389/fmars.2023.979912

OPEN ACCESS

EDITED BY
Manuel Maldonado,
Center for Advanced Studies of Blanes (CSIC), Spain

REVIEWED BY
Swee Cheng Lim,
National University of Singapore, Singapore
Pilar Ríos,
Spanish Institute of Oceanography, Spain
Laia Leria,
Centro de Estudios Avanzados de Blanes (CEAB-CSIC), Spain

*CORRESPONDENCE
Xinzheng Li
lixzh@qdio.ac.cn

†These authors have contributed equally to this work

SPECIALTY SECTION
This article was submitted to Marine Evolutionary Biology, Biogeography and Species Diversity, a section of the journal Frontiers in Marine Science

RECEIVED 04 July 2022
ACCEPTED 25 January 2023
PUBLISHED 09 February 2023

CITATION
Gong L, Yang M, Janussen D, Dohrmann M and Li X (2023) A new species of *Caulophacus* (Hexactinellida: Lyssacinosida: Rossellidae) from the western Pacific Ocean, with new insights into the mitochondrial genome characteristics of hexactinellid sponges. *Front. Mar. Sci.* 10:979912. doi: 10.3389/fmars.2023.979912

A new species of *Caulophacus* (Hexactinellida: Lyssacinosida: Rossellidae) from the western Pacific Ocean, with new insights into the mitochondrial genome characteristics of hexactinellid sponges

Lin Gong[1,2†], Mei Yang[1,2†], Dorte Janussen[3], Martin Dohrmann[4] and Xinzheng Li[1,2,5,6*]

[1]Institute of Oceanology, Chinese Academy of Sciences, Qingdao, China, [2]Center for Ocean Mega-Science, Chinese Academy of Sciences, Qingdao, China, [3]Abteilung Marine Zoologie, Forschungsinstitut und Naturmuseum Senckenberg, Frankfurt, Germany, [4]Independent Researcher, Munich, Germany, [5]Laboratory for Marine Biology and Biotechnology, Qingdao National Laboratory for Marine Science and Technology, Qingdao, China, [6]Graduate University, University of Chinese Academy of Sciences, Beijing, China

A new species, belonging to the rossellid subfamily Lanuginellinae Gray, 1872, is described based on two specimens collected from two different seamounts in the western Pacific Ocean. Species characterization was approached by analyzing the morphological and skeletal features as well as the complete mitochondrial genome. *Caulophacus* (*Caulodiscus*) *iocasicus* sp. nov. is distinguishable from its congeners by its branched external shape and a unique combination of microscleres. It only has hemionychohexasters while other *C.* (*Caulodiscus*) species additionally have either onychohexasters or discohexasters. Furthermore, the new species has microhexactins, which have not been reported from the other six species of *C.* (*Caulodiscus*). Regarding the mitochondrial genome, the occurrence of the *atp8* gene, the absence of *tRNA* ^{E}, the translocation of *tRNA* ^{D} between *cob* and *nad6*, and the rearrangement of *nad6-nad4* distinguish the new species from other rossellids and even other hexactinellids for which mitogenomic information is available. The herein revised morphological and molecular information of the genus *Caulophacus* also suggests that the monospecific subgenus *C.* (*Caulophacella*) should be removed from *Caulophacus* and reinstated as a separate genus in the subfamily Lanuginellinae.

KEYWORDS

Porifera, Caulophacus (Caulodiscus) iocasicus sp. nov., Caulophacella, seamount, mitochondrial genome

Introduction

Caulophacus Schulze, 1886 is a pedunculate genus within Lanuginellinae Gray, 1872, with 32 species currently recognized (de Voogd et al., 2022). *Caulophacus* is cosmopolitan (Figure 1), with species recorded from the Pacific, Atlantic, and Indian oceans (Supplementary Excel S1). It is essentially a deep-sea genus. *Caulophacus* (*Caulodiscus*) *leonieae* Buskowiak & Janussen, 2021 is reported to live at a depth of 296 m, which is the shallowest recorded depth for the genus. Generally, only a few species are reported to occur in the mesobenthic zone (200–1000 m), while most of the species occur in bathyal (1000–4000 m) and abyssal (4000–6000 m) waters. The deepest record for *Caulophacus* has been, until now, 6770 m (hadal), held by *Caulophacus* (*Caulophacus*) *hadalis* Lévi, 1964. The highest abundance of *Caulophacus* tends to be reported at depths of 3000–5000 m. Some species have a large depth range, such as *C. (Caulophacus) latus* Schulze, 1886, from 2926 m (Schulze, 1887) to 6710 m (Koltun, 1970).

Caulophacus once contained two subgenera (*C.* (*Caulophacus*) Schulze, 1886 and *C.* (*Caulodiscus*) Ijima, 1927) (Tabachnick, 2002). Janussen et al. (2004) established a new subgenus *C.* (*Oxydiscus*) based on specimens from the Weddell Sea, which is characterized by microscleres having oxyoidal and discoidal endings. They suggested the rossellid genus *Caulophacella* Lendenfeld, 1915 should be included in *Caulophacus* as another subgenus with microscleres having exclusively oxyoidal endings, which was formally implemented by Boury-Esnault et al. (2015). Therefore, there are currently 4 subgenera of *Caulophacus*, which are differentiated by the terminations of microscleres: *C.* (*Caulodiscus*) having discoidal and onychoidal terminations, *C.* (*Caulophacella*) having exclusively oxyoidal terminations, *C.* (*Caulophacus*) mainly having discoidal terminations, and *C.* (*Oxydiscus*) having oxyoidal and discoidal terminations (Tabachnick, 2002; Janussen et al., 2004). However, molecular phylogenetic analyses indicate that inclusion of *Caulophacella* in *Caulophacus* is not justified and that *C.* (*Caulodiscus*) and *C.* (*Caulophacus*) are not monophyletic groups (Dohrmann et al., 2008; Dohrmann et al., 2017; Kersken et al., 2018; Dohrmann, 2019). Thus, the intrageneric classification scheme of *Caulophacus* requires revision based on morphological and molecular data.

Mitochondria play important roles in providing energy for eukaryotic cells. Genetic-level changes in mitochondria can reflect physiological changes and evolutionary pressures of the species (Plese et al., 2021). Moreover, mitochondria have their own genetic system, which contains useful information for investigating phylogenetic relationships. The mitogenome of most metazoans is a closed circular molecule of 15–20 kb in length, usually containing 37 genes: 13 protein-coding genes (PCGs), 2 ribosomal RNA (rRNA) genes, and 22 transfer RNA (tRNA) genes (Boore, 1999). However, the mitogenome characteristics of sponges differ between classes. For example, Demospongiae and Homoscleromorpha have 14 PCGs (Gazave et al., 2010; Ereskovsky et al., 2017; Plese et al., 2021), Hexactinellida have 13 PCGs (*atp8* missing) (Haen et al., 2014), and Calcarea have 11 PCGs (*atp8*, *nad6*, and *nad4L* missing) (Lavrov et al., 2016). To date, only a few mitochondrial genomes of hexactinellid sponges have been sequenced. Most of the mitogenome sequences are incomplete and only those of four species are complete (*Aphrocallistes vastus*, *Vazella pourtalesii*, *Tabachnickia* sp., and *Lophophysema eversa*). We analyzed the incomplete and complete mitogenomes of hexactinellid sponges available in GenBank, which range from 13,588 bp to 20,591 bp in length and contain 1–2 rRNA genes, 10–14 PCGs and 11–22 tRNA genes. Many important taxa of hexactinellid sponges still lack mitochondrial genomes, and deeper phylogenetic relationships could be investigated with more comprehensive taxon sampling.

In 2017 and 2019, we conducted cruises to two different seamounts in the northwestern Pacific Ocean to survey seamount biodiversity with the research vessel *Ke Xue*. Two remarkable bush-like sponge specimens were collected at depths of 884 m and 1055.5 m, respectively. Based on the morphological and molecular analyses, they are described and illustrated herein as new to science. We also report the complete mitogenome of the new species and we hope to broaden our view on the diversity of mt genomes through the first mt genome of *Caulophacus*.

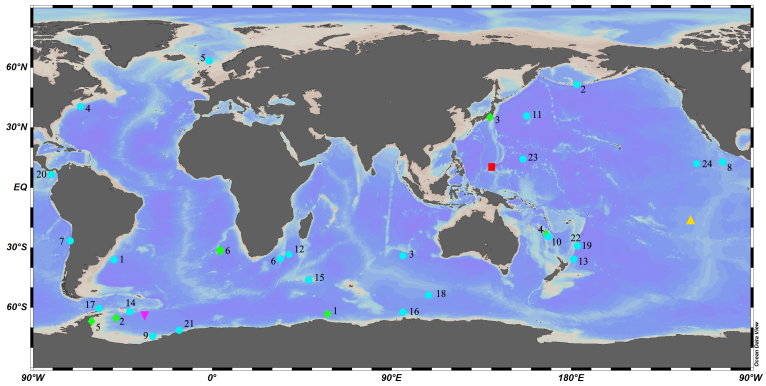

FIGURE 1
Global diversity of *Caulophacus*: ▲ *Caulophacus (Caulophacella) tenuis*. ▼ *Caulophacus (Oxydiscus) weddelli*. ◆ *Caulophacus (Caulodiscus)*: 1, *C. valdiviae*; 2, *C. brandti*; 3, *C. lotifolium*; 4, *C. onychohexactinus*; 5, *C. leonieae*; 6, *C. polyspiculus*. ● *Caulophacus (Caulophacus)*: 1, *C. abyssalis*; 2, *C. adakensis*; 3, *C. antarcticus*; 4, *C. agassizi*; 5, *C. arcticus*; 6, *C. basispinosus*; 7, *C. chilense*; 8, *C. cyanae*; 9, *C. discohexactinus*; 10, *C. discohexaster*; 11, *C. elegans*; 12, *C. galatheae*; 13, *C. hadalis*; 14, *C. instabilis*; 15, *C. latus*; 16, *C. oviformis*; 17, *C. palmeri*; 18, *C. pipetta*; 19, *C. ramosus*; 20, *C. schulzei*; 21, *C. scotiae*; 22, *C. serpens*; 23, *C. variens*; 24, *C. wilsoni*. ■ *Caulophacus (Caulodiscus) iocasicus* sp. nov.

Materials and methods

Sample collection

The specimens were collected from two seamounts by the submersible ROV *Fa Xian* with the R/V *Ke Xue* during its cruises in 2017 and 2019 in the western Pacific Ocean, and preserved in 75% ethanol. The samples are deposited in the Marine Biological Museum (MBM) of the Chinese Academy of Sciences, Qingdao, China.

Spicule analysis

Concentrated nitric acid was used to digest a small piece of sponge tissue and clean spicules were isolated by rinsing several times with distilled water and dehydrated with 95% ethanol. A Hitachi S-3400N scanning electron microscope (SEM) was used to observe the spicules. Additional spicule measurements were performed using an Olympus DSX500 Optodigital light microscope (LM) (Table 1).

DNA extraction and PCR amplification

Total genomic DNA was extracted using a Tissue DNA Kit (OMEGA Bio-Tek) following the manufacturer's instructions. Polymerase chain reaction (PCR) reaction mix (25 µL) comprised 12.5 µL of Premix Taq™ (Takara, Otsu, Shiga, Japan), 1 µL of each primer, 2 µL of template DNA, and 8.5 µL DNase-free ddH_2O. The 16S rDNA was amplified with the primers 16S1fw/16SH_mod (Dohrmann et al., 2008). The amplification was performed using the following procedure: 5 min/94°C; 30 cycles (30 s/94°C, 30 s/48°C, 60 s/72°C); 5 min/72°C.

Illumina sequencing, mitochondrial genome assembly and annotation

Short-insert libraries (insert size of 430 bp) were constructed according to the manufacturer's instructions of the TruSeq™ Nano DNA Sample Prep Kit (Illumina) and sequenced on an Illumina HiSeq 4000 instrument (San Diego, USA). Quality control of the raw data was performed using Trimmomatic (Bolger et al., 2014) by removing adapters, duplicated sequences, reads with a quality score below 20 (Q < 20), and reads containing a percentage of uncalled bases ("N" characters) equal to or greater than 10%. Clean data were reconstructed using a combination of *de novo* and reference-guided assemblies. *De novo* assembly with GetOrganelle v1.6.4 (Jin et al., 2020) was performed using the mitochondrial genome of *Vazella pourtalesii* (NC_028054.1) as the reference. Potential mitochondrial reads were extracted from the Illumina reads using BLAST (https://blast.ncbi.nlm.nih.gov/Blast.cgi). The filtered reads were assembled into contigs using SPAdes-3.13.1 (Bankevich et al., 2012). Finally, the assembled sequence was reordered and oriented according to the reference mitochondrial genome, thus generating the final assembled sequence. The mitochondrial genes were annotated using the MITOS2 webserver (Bernt et al., 2013). Locations and sizes of the protein coding genes (PCGs) were identified using Open Reading Frame Finder (http://www.ncbi.nlm.nih.gov/gorf/gorf.html) with the invertebrate mitochondrial code. Transfer RNA (tRNA) genes were predicted by ARWEN (Laslett & Canback, 2008) and DOGMA (Wyman et al., 2004). Ribosomal RNA (rRNA) genes were identified by the rRNAmmer 1.2 webserver (Lagesen et al., 2007). The mitochondrial genome map was generated by CGView (Stothard & Wishart, 2005). Nucleotide composition and codon usage were calculated using DnaSP 5.1 (Librado & Rozas, 2009). The values of AT and GC skews were calculated according to the following formulas: AT skew = (A − T)/(A + T) and GC skew = (G − C)/(G + C) (Perna & Kocher, 1995). The relative synonymous codon usage (RSCU) data were obtained with MEGA 7 (Kumar et al., 2016).

Phylogenetic analysis

A phylogenetic tree was reconstructed from partial 16S rDNA and COI gene sequences of Lanuginellinae. We obtained 11 16S rDNA sequences and 7 COI sequences of Lanuginellinae from GenBank, including all four subgenera of *Caulophacus*. *Rossella levis* was used as an outgroup (Table 2).

We used the workflow desktop platform of PhyloSuite (Zhang et al., 2020) to build the phylogenetic tree. The sequences were aligned using MAFFT (Katoh & Standley, 2013) with the default parameters. The concatenated dataset consisted of 1052 bp (16S/COI = 493/559bp). The best-fitting nucleotide substitution model, which was determined by ModelFinder 2 (Kalyaanamoorthy et al., 2017) with the BIC (Bayesian Information Criterion), was GTR+F+G4. Bayesian inference (BI) analysis was carried out in MrBayes 3.2 (Ronquist et al., 2012) with Markov Chains run for 2 million generations, sampling every 1000 generations. The first 25% of trees were discarded as burn-in. The average standard deviation of split frequencies reached 0.0045. Phylogenetic trees were annotated in iTOL (Letunic & Bork, 2021; https://itol.embl.de/).

We also built a phylogeny based on the 14 PCGs of mitochondrial sequences, also using PhyloSuite. We downloaded 13 relatively complete or complete mitogenomes of hexactinellid sponges belonging to two subclasses, three orders, and seven families (Table 2). Alignments were built in MAFFT. GBlocks v0.91b (Castresana, 2000) was used to eliminate ambiguously aligned regions and gaps of each gene. Then the trimmed alignments were concatenated into a single dataset using the Concatenate Sequence function in PhyloSuite. For BI and Maximum Likelihood (ML) analyses, the best-fit substitution models and partition schemes were inferred by ModelFinder (Kalyaanamoorthy et al., 2017) (Supplementary Table S1). Maximum likelihood (ML) analysis was performed in IQ-TREE 1.6.10 (Nguyen et al., 2015). Topological robustness for the ML analysis was evaluated with 1000 bootstrap replicates. Bayesian inference was conducted in MrBayes 3.2, using four chains run for 10 million generations, sampling every 1000 generations and discarding the first 25% of samples as burn-in.

10.3389/fmars.2023.979912

TABLE 1 Measurements of the spicules of *Caulophacus (Caulodiscus) iocasicus* sp. nov. (in μm); "n", number of spicules measured; "s.d.", standard deviation; "range", range from the minimum to the maximum.

	n	mean	range	
dermalia, pinular hexactins				
pinular ray length	20	440	340–521	35
pinular ray width	20	16	13–19	1.8
proximal ray length	20	136	119–155	8.5
proximal ray width	20	13	11–17	1.8
tangential ray length	20	153	112–196	27
tangential ray width	20	13	10–15	1.3
hypodermalia, pentactins				
tangential ray length	20	442	195–753	121.5
tangential ray width	20	20	15–28	3.1
atrialia, pinular hexactins				
pinular ray length	20	157	84–247	50
pinular ray width	20	19	16–22	1.7
proximal ray length	20	106	69–153	19
proximal ray width	20	15	11–18	1.5
tangential ray length	20	146	105–184	20.5
tangential ray width	20	15	11–18	1.8
hypoatrialia, pentactins				
tangential ray length	20	527	314–687	95
tangential ray width	20	25	22–29	2.2
choanosomalia, diactins				
length	20	1813	796–3057	641
width	20	9	7–13	1.3
choanosomalia, hexactins				
ray length	20	598	363–869	134
ray width	20	19	15.9–22.5	1.9
microhexactins				
length	9	123	97–168	25.4
width	9	7.2	6.1–8.5	0.8
discohexactins				
ray length	20	70	57–86	6.7
ray width	20	4.6	3.9–5.6	0.5
onychohexactins				
ray length	20	48	38–61	6.2
ray width	20	3.1	2.5–3.7	0.3
hemionychohexasters				
diameter	11	99	78–122	11.2

Results

Taxonomy

Family Rossellidae Schulze, 1885
Subfamily Lanuginellinae Gray, 1872
Genus Caulophacus Schulze, 1886
Subgenus Caulophacus (*Caulodiscus*) Ijima, 1927
Caulophacus (*Caulodiscus*) *iocasicus* Gong & Li, **sp. nov.**
(Figures 2, 3, Table 1)
ZooBank registration LSID: urn:lsid:zoobank.org:act:0A0CB816-1E8B-485A-91C3-AEDA19A0B762

Material examined

Holotype

MBM287354, Caroline seamount located south of the Mariana Trench and north of the Yap Trench (10°30'58.559''N, 140° 10'23.238''E), Pacific Ocean, 25 August 2017, 1055.5 m depth.

Paratype

MBM287355, Mariana M5 seamount near Mariana Trench (10° 04'40.001''N, 140°11'57.426''E), Pacific Ocean, 28 May 2019, 884 m depth.

Description

The new species has 8–10 branches like a luxuriant tree growing on the bottom of the sea. There is a mushroom-shaped body at the end of each branch. The holotype has 8 mushroom-shaped spheres (Figures 2A, C). The overall dimension of each sphere ranges from 38 mm to 170 mm in diameter. The sponge is approximately 110 cm in height with a main stalk having a diameter of 17 mm and many stems having a thinnest diameter of 6 mm. The lateral stalks can be as strong as the main stalk and the length of each lateral stalk varies from 19 mm to 65 mm. The paratype has 10 spheres (Figures 2B, D) with diameters ranging from 40 mm to 160 mm. The sponge is approximately 120 cm in height, with a prominent main stalk having a diameter of 16 mm. The stalks of the sponge are hollow and there are no visible spicules on the surface. Color of the body in life is white and pale brown when preserved in ethanol.

Dermalia are pinular hexactins (Figure 3D), with pinular ray gradually tapering towards the end (340–(440)–521 μm in length), slightly spiny tangential rays 112–(153)–196 μm in length, and proximal ray 119–(136)–155 μm in length. Atrialia are pinular hexactins (Figure 3C) with spindle-like pinular ray (84–(157)–247 μm in length). The tangential and proximal rays, covered with many small spines, are 105–(146)–184 μm and 69–(106)–153 μm in length, respectively. Hypodermalia (Figure 3A) and hypoatrialia (Figure 3B) are pentactins with smooth rays. Tangential rays of hypodermalia and hypoatrialia are 195–(442)–753 μm and 314–(527)–687 μm in length, respectively. The length of the proximal ray is difficult to measure under a light microscope. Choanosomal spicules are diactins and hexactins. Diactins (796–(1813)–3057 μm in length; 7–(9)–13 μm in width) are smooth with sparsely spined bluntly conical terminations (Figure 3E). Hexactins (363–(598)–869 μm in length; 15.9–(19.4)–22.5 μm in width) are smooth with conical terminations.

Microscleres are discohexactins, onychohexactins, hemionychohexasters and microhexactins. Discohexactins (Figure 3G) have six slightly curved rays (57–(70)–86 μm in length; 3.9–(4.6)–5.6 μm in width) covered with numerous spines (Figure 3J). Most of the onychoidal microscleres are onychohexactins (Figure 3H) with rays covered with small spines (Figure 3K). The ray length of onychohexactins is 38–(48)–61 μm and the width is 2.5–(3.1)–3.7 μm.

TABLE 2 16S rDNA, COI, and mitochondrial genome sequences used in this study.

Species	GenBank accession numbers		Species	GenBank accession numbers
	16S rDNA	COI		mitochondrial genomes
Caulophacus valdiviae	AM886348.1	FR848929.1	*Iphiteon panicea*	EF537576.1
Caulophacus weddelli	AM886349.1	FR848928.1	*Sympagella nux*	EF537577.1
Caulophacus arcticus	AM886350.1	FR819684.1	*Bathydorus laniger*	KJ634155.1
Caulophacella tenuis	AM886351.1	FR848927.1	*Docosaccus maculatus*	KJ634156.1
Caulophacus variens	MF683994.1		*Lophophysema eversa*	KM035411.1
Caulophacus sp. (SMF12065)	MF683996.1		*Aphrocallistes beatrix*	KM580069.1
Caulophacus sp. SMF12088	MF683993.1		Euretidae gen. sp. (DVL-2014)	KM580070.1
Caulophacus sp. (SMF11691)	MF683995.1		*Hertwigia falcifera*	KM580071.1
Doconesthes dustinchiversi	LT627517.1	LT627550.1	Rossellidae sp. (DVL-2014)	KM580073.1
Lophocalyx profundum	AM886352.1	FR848926.1	*Tabachnickia* sp. (DVL-2014)	KM580074.1
Lophocalyx sp. (SMF12066)	MF683997.1		*Aphrocallistes vastus*	NC_010769.1
Rossella levis	HE580201.1	HE580223.1	*Vazella pourtalesii*	NC_028054.1
Caulophacus (*Caulodiscus*) *iocasicus* (holotype)	ON229907	ON764414	*Oopsacas minuta*	NC_027419.1
Caulophacus (*Caulodiscuss*) *iocasicus* (paratype)	ON229908		*Caulophacus* (*Caulodiscus*) *iocasicus*	ON764414

10.3389/fmars.2023.979912

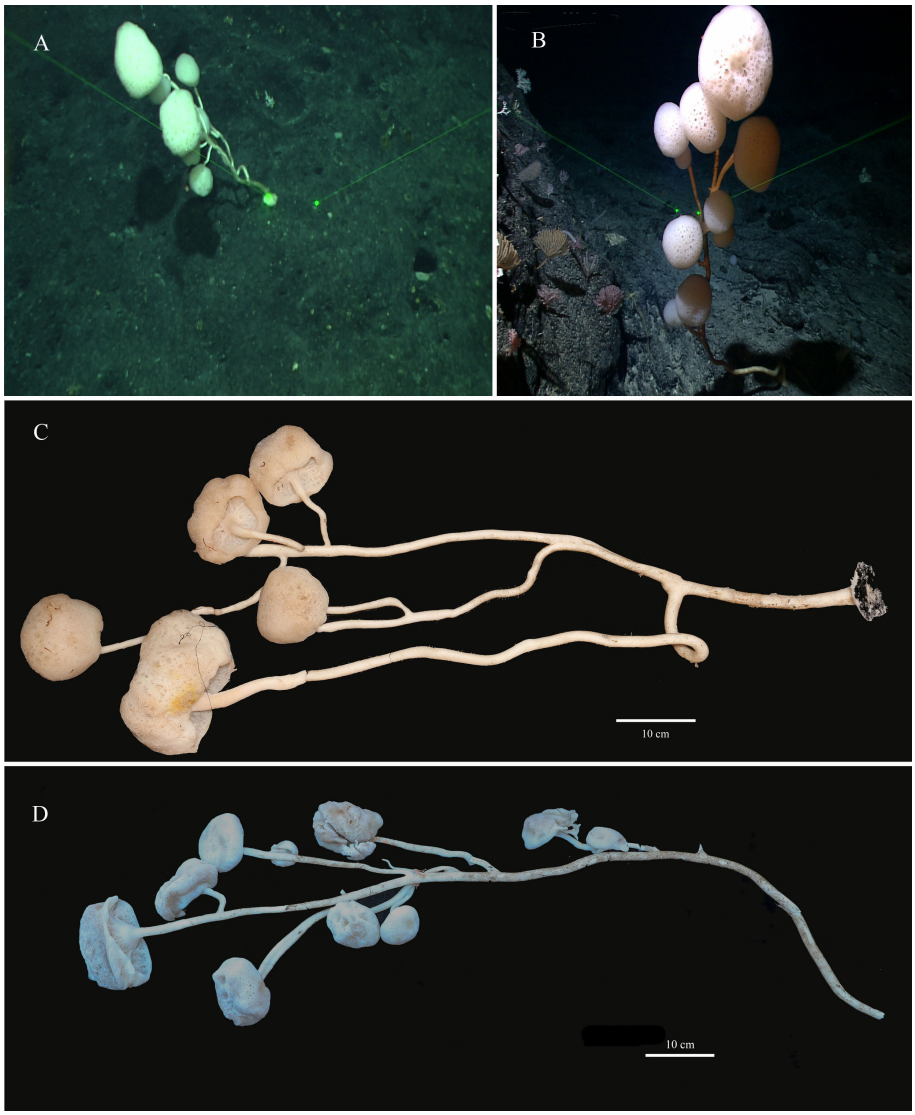

FIGURE 2
Caulophacus (*Caulodiscus*) *iocasicus* sp. nov. **(A)**, photograph showing the holotype specimen in its natural habitat. **(B)**, photograph showing the paratype specimen in its natural habitat. **(C)**, external morphology of the holotype after removal from seawater. **(D)**, external morphology of the paratype after removal from seawater.

Hemionychohexasters (Figure 3I) are 78–(99)–122 μm in diameter. Microhexactins (Figure 3F) with smooth rays (97–(123)–168 μm in length and 6.1–(7.2)–8.5 μm in width) occur infrequently.

Etymology

iocasicus is named after iocas, celebrating the 70th anniversary of the Institute of Oceanology, Chinese Academy of Sciences (IOCAS) from its establishment in 1950.

Type locality

Seamounts near Mariana Trench and Yap Trench (western Pacific) with hard bottom, 884–1055.5 m.

Mitochondrial genome organization and characterization

The complete mitogenome of *C.* (*Caulodiscus*) *iocasicus* sp. nov. is 19,930 bp in length. The genome encodes 37 genes, including 14 PCGs, 2 rRNA genes, and 21 tRNA genes (duplication of $tRNA^{Leu}$ and $tRNA^{Ser}$) (Figure 4). All of the genes are encoded on the heavy (H) strand. There were 5 overlaps between adjacent genes with a size range of 3 to 83 bp (Table 3). The combined length of 14 PCGs was 12,041 bp, accounting for 60.42% of the complete mitochondrial genome. Two of the PCGs started with ATA as initiation codons, while the others started with ATG. All of the PCGs ended with TAA as the stop codon (Table 3). The 14 PCGs encode a total of 4,033 amino acids, Met (12.77%) and Cys (0.92%) are the most and the least frequently used amino acids, respectively (Figure 5). The relative synonymous codon usage (RSCU) values show that the six most commonly used codons are AGA (Ser), GUA (Val), CGA (Arg), GGA

(Gly), UUA (Leu), and CUA (Leu) (Figure 5), all of which have A in their third codon position. These features are similar to many metazoans, where codon usage is biased toward A and T at the third codon position (Zhang et al., 2017; Yang et al., 2019). The lengths of the 21 tRNA genes range from 63 ($tRNA^{Met}$) to 73 bp ($tRNA^{Ser\ (AGA)}$), and all tRNAs can be folded into classic clover leaf structures (Supplementary Figure S1). The rRNA genes of rrnS and rrnL of the new species are 940 bp and 1493 bp in length, respectively (Table 3).

Phylogenetic analysis

16S rDNA and COI gene phylogeny

In the BI tree (Figure 6) based on the 16S rDNA and COI sequences, *C.* (*Caulodiscus*) *iocasicus* sp. nov. is nested within the genus *Caulophacus,* confirming the validity of our genus assignment. The new species is not closely related to *C.* (*Oxydiscus*), and relationships to *C.* (*Caulodiscus*) or *C.* (*Caulophacus*) are not resolved. *Caulophacella* groups outside of *Caulophacus*, as sister to all other Lanuginellinae included here. This is different from previous studies that resolved a closer relationship of *Caulophacella* to *Doconesthes* and *Lophocalyx* (Dohrmann et al., 2017; Kersken et al., 2018; Dohrmann, 2019).

Mitochondrial protein-coding gene phylogeny

The mitogenomic phylogenetic tree based on the nucleotide sequences of 14 PCGs (Supplementary Figure S2) is consistent with previous works (e.g., Haen et al., 2014; Dohrmann, 2019). The new species is nested within the family Rossellidae as sister to the other included lanuginelline, *Sympagella nux*.

Mitochondrial gene order and rearrangements

The mitogenome of *C.* (*Caulodiscus*) *iocasicus* sp. nov. contains *atp9*, which has only been found in sponges among Metazoa (Haen et al., 2007). The new species is only the second species with *atp8*, which is lacking in most of the hexactinellid sponges investigated so far (except *Oopsacas minuta* (Jourda et al., 2015)). Additionally, it misses $tRNA^{E}$, unlike other rossellids. The gene orders vary considerably among hexactinellid sponges, while the more closely related taxonomic groups are generally stable (Figure 7). Within Rossellidae, the orders of protein coding genes are generally conserved except for the absence of *nad6* in most species. Transposition of *nad4* and *nad6* occurred in the two completed sequences of *V. pourtalesii* and the new species. In rossellid sponges, two conserved gene clusters are shared: *M–Q–rrnS–rrnL–*

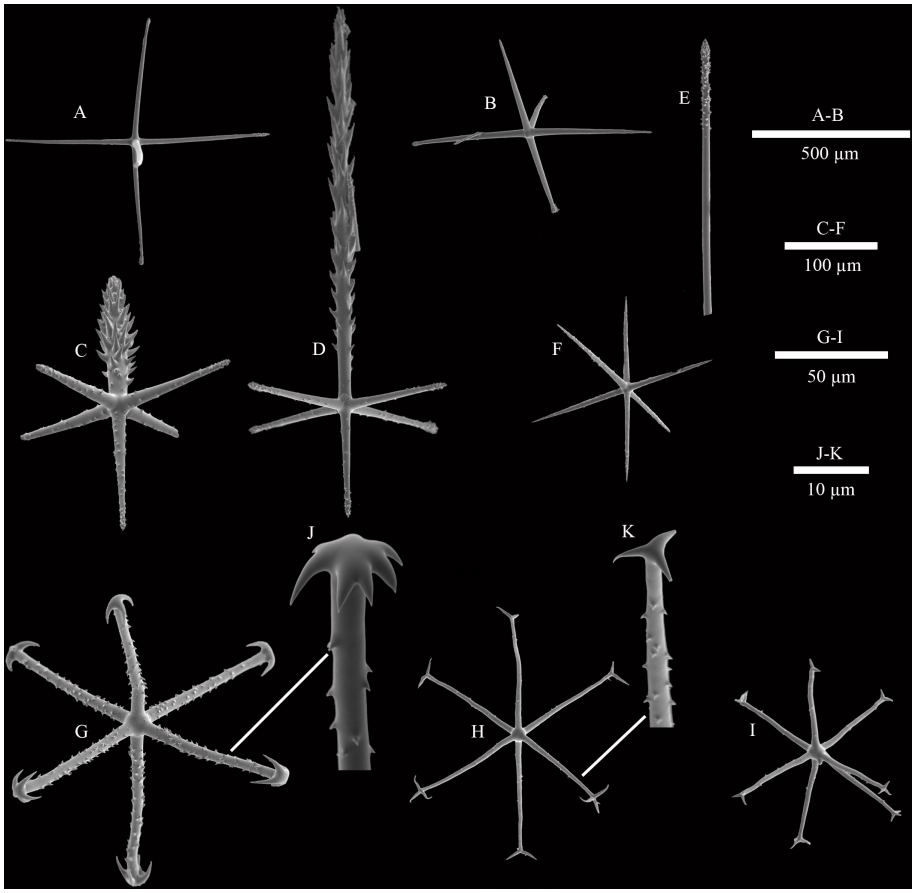

FIGURE 3
SEM images of spicules of *Caulophacus* (*Caulodiscus*) *iocasicus* sp. nov. **(A)**, hypodermal pentactin; **(B)**, hypoatrial pentactin; **(C)**, atrial pinular hexactin; **(D)**, dermal pinular hexactin; **(E)**, details of the termination of choanosomal diactin; **(F)**, microhexactin; **(G)**, discohexactin; **(H)**, onychohexactin; **(I)**, hemionychohexaster; **(J)**, detail of the toothed disc of discohexactin; **(K)**, detail of the termination of onychohexactin.

10.3389/fmars.2023.979912

TABLE 3 Mitogenome organization of *Caulophacus* (*Caulodiscus*) *iocasicus* sp. nov.

Name	Strand	Range	Size		Codon			Intergenic nucleotides
			Nucleotides	Amino acid	Start	Stop	Anticodon	
cox1	+	1-1575	1575	524	ATG	TAA		7
trnT	+	1556-1624	69				TGT	-20
atp8	+	1625-1768	144	47	ATG	TAA		0
atp9	+	1960-2199	240	49	ATG	TAA		191
trnV	+	2214-2281	68				TAC	14
trnM	+	2329-2391	63				CAT	47
trnQ	+	2392-2462	71				TTG	0
rrnS	+	2460-3399	940					-3
rrnL	+	3572-5064	1493					172
$trnS2^{tca}$	+	5073-5142	70				TGA	8
$trnS1^{aga}$	+	5156-5228	73				TCT	13
cox2	+	5238-5966	729	242	ATG	TAA		9
trnA	+	6049-6119	71				GCT	82
trnP	+	6133-6198	66				TGG	13
trnR	+	6199-6269	71				TCG	0
trnK	+	6283-6349	67				TTT	13
nad3	+	6353-6712	360	119	ATG	TAA		3
trnW	+	6730-6798	69				TCA	17
$trnL1^{cta}$	+	6804-6871	68				TAG	5
nad4l	+	6873-7175	303	100	ATG	TAA		1
atp6	+	7182-7910	729	242	ATG	TAA		6
cox3	+	7911-8693	783	260	ATG	TAA		0
nad2	+	8931-10160	1230	409	ATA	TAA		237
nad5	+	10141-11946	1806	601	ATA	TAA		-20
trnF	+	11922-11992	71				GAA	-25
trnC	+	11993-12064	72				GCA	0
nad1	+	12072-13106	1035	344	ATG	TAA		7
$trnL2^{tta}$	+	13024-13090	67				TAA	-83
trnI	+	13092-13159	68				GAT	1
trnN	+	13161-13230	70				GTT	1
trnY	+	13236-13304	69				GTA	5
cob	+	13308-14477	1170	389	ATG	TAA		3
trnD	+	14512-14580	69				TCA	34
nad6	+	15158-15688	531	176	ATG	TAA		577
nad4	+	16128-17633	1506	501	ATG	TAA		439
Control regiojn	+	17634-19756	2123					0
trnG	+	19757-19824	68				TCC	0
trnH	+	19855-19923	69				GTG	30

10.3389/fmars.2023.979912

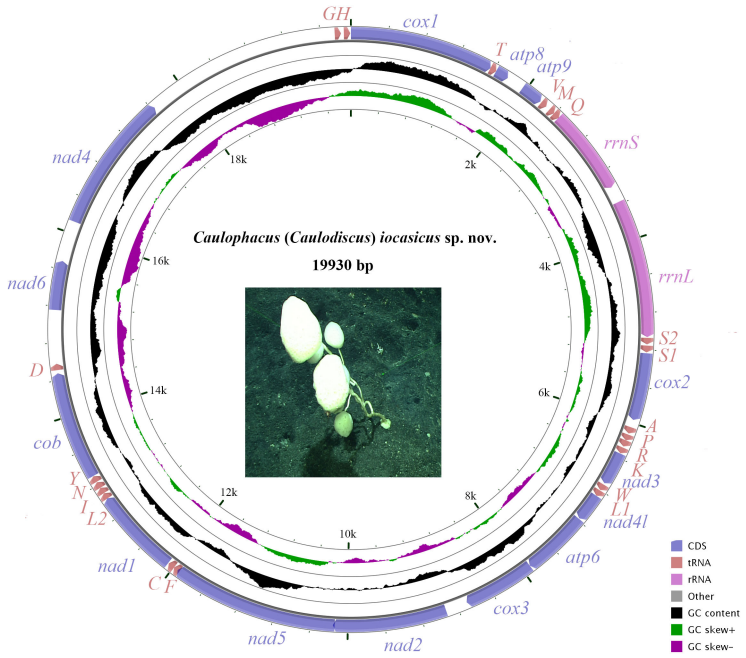

FIGURE 4
The organization of the mitochondrial genome of *Caulophacus* (*Caulodiscus*) *iocasicus* sp. nov. Genes for protein coding genes are shown with standard abbreviations. 12S and 16S ribosomal RNA genes are are indicated as *rrnS* and *rrnL*, respectively. Genes for tRNAs are labeled by one-letter code for their corresponding amino acid.

S2 and *K–nad3–W–L1–nad4–atp6–cox3–nad2–nad5–F–C–nad1–L2–I–N*. Although most of the gene sequences are incomplete, we can see a gene rearrangement of $tRNA^D$ in the new species.

Discussion

Morphological differences

The new species is attributed to the genus *Caulophacus* by having long peduncles, dermalia and atrialia being pentactins and hexactins, and microscleres having discoidal and onychoidal terminations. The most outstanding character of the new species is its external shape with many branches. Other pedunculate branched *Caulophacus* only have small branches, such as *C.* (*Caulophacus*) *ramosus* Reiswig, Dohrmann & Kelly, 2021. However, their spicules are very different. *Caulophacus (Caulophacus) ramosus* has thin-rayed stellate discohexasters and lacks onychohexasters (Reiswig et al., 2021).

The new species is assigned to *C.* (*Caulodiscus*) by having microscleres with discoidal and onychoidal terminations. Two of

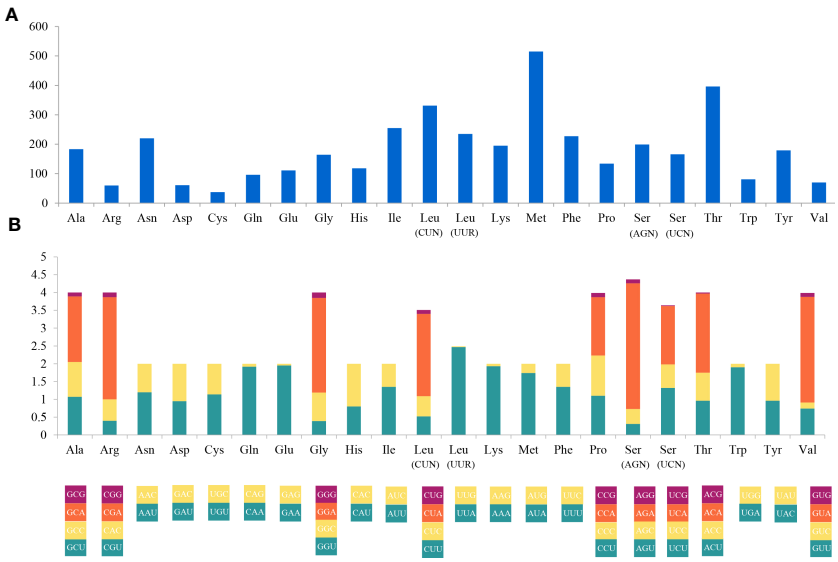

FIGURE 5
Codon usage **(A)** and the relative synonymous codon usage (RSCU) **(B)** of the *Caulophacus* (*Caulodiscus*) *iocasicus* sp. nov. mitogenome. Numbers to the left refer to the total number of codons **(A)** and the RSCU values **(B)**.

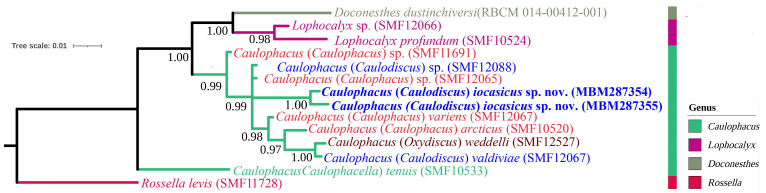

FIGURE 6
Phylogenetic tree obtained by Bayesian inference analysis based on 16S rDNA and COI gene sequences. The numbers at each node are Bayesian posterior probabilities (PP).

the six described species of *C.* (*Caulodiscus*) have onychohexasters (*C.* (*Caulodiscus*) *onychohexactinus* Tabachnick & Lévi, 2004 and *C.* (*Caulodiscus*) *lotifolium* Ijima, 1903), and the other four species have discohexasters, while the new species only has hemionychohexasters. It also has microhexactins, which were not found in other *C.* (*Caulodiscus*) species. Therefore, the unique combination of microscleres justifies the proposal that the species is new to science. Another distinctive characteristic of the new species is the multiramose body shape, unknown from other *C.* (*Caulodiscus*) species, which only have a single unbranched peduncle.

Molecular data

Molecular data show that the new species does not appear to be closely related to any of the included *C.* (*Caulophacus*) or *C.* (*Caulodiscus*) species. However, both of these subgenera are polyphyletic groups in the molecular phylogeny. Increased taxon sampling of *Caulophacus* for molecular phylogenetics combined with thorough morphological revision will be necessary to resolve its internal relationships and propose a natural subgeneric classification of this large genus.

FIGURE 7
Mitochondrial gene organization and gene rearrangement in Hexactinellida. The length of mitochondrial genomes is presented in brackets. Conserved gene blocks within Rossellidae are shown in pink line; gene arrangements of $tRNA^{D}$ within Rossellidae are shown as green triangles; *=atp8* genes are shown as blue triangles.

Establishment of the genus *Caulophacella*

In molecular phylogenies, *C.* (*Caulophacella*) does not nest within the clade of *Caulophacus* (Dohrmann et al., 2017; Kersken et al., 2018; Dohrmann, 2019; this study: Figure 6). Also, all *Caulophacus* species have discoidal microscleres, except for *C.* (*Caulophacella*) *tenuis*. Therefore, we remove *Caulophacella* from *Caulophacus* and reinstate it as a separate genus in the subfamily Lanuginellinae, reversing the move of Boury-Esnault et al. (2015).

Conclusion

Caulophacus species are mostly deep-sea dwellers, and their richest abundance is at depths of 3000–5000 m. *Caulophacus* (*Caulodiscus*) *iocasicus* sp. nov. is reported from depths of 884–1055.5 m, somewhat shallower than most species (Supplementary Excel S1). The new species has a highly branched stalk with many mushroom-shaped bodies while most of its congeners only have a single unbranched stalk. Also, its spicule composition is unique among *C.* (*Caulodiscus*).

The complete mitogenome of the new species has 14 PCGs, 2 rRNA genes, and 21 tRNA genes. It is the second hexactinellid genome that contains *atp8*, but it lacks $tRNA^{E}$, which is reported from all other rossellids investigated so far. A higher taxon coverage of mitogenomes will be needed to explore the mitochondrial characteristics of Rossellidae and to obtain a more comprehensive understanding of *Caulophacus*.

Caulophacus (*Caulophacella*) does not group within *Caulophacus* in molecular phylogenies and lacks discoidal microscleres, which are always present in the other subgenera. Therefore, we reinstate it as a separate genus in the subfamily Lanuginellinae.

Data availability statement

The datasets presented in this study can be found in online repositories. The names of the repository/repositories and accession number(s) can be found in the article/Supplementary Material.

Author contributions

LG drafted the manuscript. MY conducted the analysis of the mitochondrial genome. DJ and MD supervised the identification of the new species from morphology and molecular data, respectively. MD revised and edited the manuscript. XL designed the study and revised the manuscript. We confirm that all the listed authors have participated actively in the study, and have seen and approved the submitted manuscript. The authors declare that they have no conflict of interest. All authors contributed to the article and approved the submitted version.

Funding

This work was supported by the Senior User Project of RV KEXUE (KEXUE2020GZ01) and the Biological Resources Program, Chinese Academy of Sciences (No. KFJ-BRP-017-37).

Acknowledgments

Special thanks to Dr. Kuidong Xu (Institute of Oceanology, Chinese Academy of Sciences, Qingdao) for providing the deep-sea sponge specimens and the *in situ* pictures. We are grateful for the crews of the R/V 'Kexue' for their support in collecting the deep-sea sponge specimens during the cruises. We sincerely express our gratitude to the editor, Prof. Manuel Maldonado, and the reviewers for investing their time to help to improve this paper.

Conflict of interest

The authors declare that the research was conducted in the absence of any commercial or financial relationships that could be construed as a potential conflict of interest.

Publisher's note

Supplementary material

The Supplementary Material for this article can be found online at: https://www.frontiersin.org/articles/10.3389/fmars.2023.979912/full#supplementary-material

References

Bankevich, A., Nurk, S., Antipov, D., Gurevich, A. A., Dvorkin, M., Kulikov, A. S., et al. (2012). SPAdes: a new genome assembly algorithm and its applications to single-cell sequencing. *J. Comput. Biol.* 19, 455–477. doi: 10.1089/cmb.2012.0021

Bernt, M., Donath, A., Jühling, F., Externbrink, F., Florentz, C., Fritzsch, G., et al. (2013). MITOS: improved *de novo* metazoan mitochondrial genome annotation. *Mol. Phylogenet. Evol.* 69, 313–319. doi: 10.1016/j.ympev.2012.08.023

Bolger, A. M., Lohse, M., and Usadel, B. (2014). Trimmomatic: A flexible trimmer for illumina sequence data. *Bioinformatics* 30, 2114–2120. doi: 10.1093/bioinformatics/btu170

Boore, J. L. (1999). Animal mitochondrial genomes. *Nucleic Acids Res.* 27, 1767–1780. doi: 10.1093/nar/27.8.1767

Boury-Esnault, N., Vacelet, J., Reiswig, H. M., Fourt, M., Aguilar, R., and Chevaldonné, P. (2015). Mediterranean hexactinellid sponges, with the description of a new *Sympagella*

species (Porifera, Hexactinellida). *J. Mar. Biol. Ass. U.K.* 95, 1353–1364. doi: 10.1017/S0025315414001891

Buskowiak, D., and Janussen, D. (2021). An exceptional occurrence of deep-sea sponges in the region of former Larsen ice shelves, Antarctic peninsula, with the description of two new species. *Mar. Biodivers.* 51, 8. doi: 10.1007/s12526-020-01134-z

Castresana, J. (2000). Selection of conserved blocks from multiple alignments for their use in phylogenetic analysis. *Mol. Biol. Evol.* 17, 540–552. doi: 10.1093/oxfordjournals.molbev.a026334

de Voogd, N. J., Alvarez, B., Boury-Esnault, N., Carballo, J. L., Cárdenas, P., Díaz, M.-C., et al. (2022) *World Porifera database*. Available at: https://www.marinespecies.org/porifera (Accessed April 8, 2022).

Dohrmann, M. (2019). Progress in glass sponge phylogenetics: a comment on Kersken et al. (2018). *Hydrobiologia* 843, 51–59. doi: 10.1007/s10750-018-3708-7

Dohrmann, M., Janussen, D., Reitner, J., Collins, A. G., and Wörheide, G. (2008). Phylogeny and evolution of glass sponges (Porifera, Hexactinellida). *Syst. Biol.* 57 (3), 388–405. doi: 10.1080/10635150802161088

Dohrmann, M., Kelley, C., Kelly, M., Pisera, A., Hooper, J. N. A., and Reiswig, H. M. (2017). An integrative systematic framework helps to reconstruct skeletal evolution of glass sponges (Porifera, Hexactinellida). *Front. Zool.* 14, 18. doi: 10.1186/s12983-017-0191-3

Ereskovsky, A. V., Richter, D. J., Lavrov, D. V., Schippers, K. J., and Nichols, S. A. (2017). Transcriptome sequencing and delimitation of sympatric *Oscarella* species (*O. carmela* and *o. pearsei* sp. nov) from California, USA. *PloS One* 12 (9), e0183002. doi: 10.1371/journal.pone.0183002

Gazave, E., Lapébie, P., Renard, E., Vacelet, J., Rocher, C., Ereskovsky, A. V., et al. (2010). Molecular phylogeny restores the supra-generic subdivision of homoscleromorph sponges (Porifera, Homoscleromorpha). *PloS One* 5 (12), e14290. doi: 10.1371/journal.pone.0014290

Gray, J. E. (1872). Notes on the classification of the sponges. *Ann. Mag. Nat. Hist.* 9 (54), 442–461. doi: 10.1080/00222937208696616

Haen, K. M., Lang, B. F., Pomponi, S. A., and Lavrov, D. V. (2007). Glass sponges and bilaterian animals share derived mitochondrial genomic features: a common ancestry or parallel evolution? *Mol. Biol. Evol.* 24 (7), 1518–1527. doi: 10.1093/molbev/msm070

Haen, K. M., Pett, W., and Lavrov, D. V. (2014). Eight new mtDNA sequences of glass sponges reveal an extensive usage of +1 frameshifting in mitochondrial translation. *Gene* 535 (2), 336–344. doi: 10.1016/j.gene.2013.10.041

Ijima, I. (1903). Studies on the Hexactinellida. Contribution III. (*Placosoma*, a new euplectellid; Leucopsacidae and Caulophacidae). *J. Coll. Sci. Imp. Univ. Tokyo* 18 (1), 1–124.

Ijima, I. (1927). "The Hexactinellida of the Siboga expedition," in *Siboga-expeditie. uitkomsten op zoologisch, botanisch, oceanographisch en geologisch gebied verzameld in nederlandsch oost-Indië 1899- 1900 aan boord H.M.* Ed. M. Weber (Leiden: E.J. Brill), 1–383.

Janussen, D., Tabachnick, K. R., and Tendal, O. S. (2004). Deep-sea Hexactinellida (Porifera) of the Weddell Sea. *Deep-Sea Res. Part II* 51, 1857–1882. doi: 10.1016/j.dsr2.2004.07.018

Jin, J. J., Yu, W. B., Yang, J. B., Song, Y., de Pamphilis, C. W., Ting-Shuang Yi, T. S., et al. (2020). GetOrganelle: a fast and versatile toolkit for accurate de novo assembly of organelle genomes. *Genome Biol.* 21, 241. doi: 10.1186/s13059-020-02154-5

Jourda, C., Santini, S., Rocher, C., Le Bivic, A., and Claverie, J. M. (2015). Mitochondrial genome sequence of the glass sponge *Oopsacas minuta*. *Genome Announc.* 3 (4), e00823–15. doi: 10.1128/genomeA.00823-15

Kalyaanamoorthy, S., Minh, B. Q., Wong, T. K. F., von Haeseler, A., and Jermiin, L. S. (2017). ModelFinder: fast model selection for accurate phylogenetic estimates. *Nat. Methods* 14 (6), 587–589. doi: 10.1038/nmeth.4285

Katoh, K., and Standley, D. M. (2013). MAFFT multiple sequence alignment software version 7: Improvements in performance and usability. *Mol. Biol. Evol.* 30 (4), 772–780. doi: 10.1093/molbev/mst010

Kersken, D., Kocot, K., Janussen, D., Schell, T., Pfenninger, M., and Arbizu., P. M. (2018). First insights into the phylogeny of deep-sea glass sponges (Hexactinellida) from polymetallic nodule fields in the Clarion-Clipperton Fracture Zone (CCFZ), northeastern Pacific. *Hydrobiologia* 811 (1), 283–293. doi: 10.1007/s10750-017-3498-3

Koltun, V. M. (1970). "Sponge fauna of the northwestern Pacific from the shallows to the hadal depths," in *Fauna of the Kurile-Kamchatka trench and its environment. Institute of oceanology of the academy of sciences of the U.S.S.R.* Ed. V. G. Bogorov (Moskwa: Akademiya Nauk SSSR), 165–221.

Kumar, S., Stecher, G., and Tamura, K. (2016). MEGA7: Molecular evolutionary genetics analysis version 7.0 for bigger datasets. *Mol. Biol. Evol.* 33, 1870–1874. doi: 10.1093/molbev/msw054

Lagesen, K., Hallin, P., Rodland, E. A., Staerfeldt, H. H., Rognes, T., and Ussery, D. W. (2007). RNAmmer: consistent and rapid annotation of ribosomal RNA genes. *Nucleic. Acids Res.* 35, 3100–3108. doi: 10.1093/nar/gkm160

Laslett, D., and Canback, B. (2008). ARWEN: a program to detect tRNA genes in metazoan mitochondrial nucleotide sequences. *Bioinformatics* 24, 172–175. doi: 10.1093/bioinformatics/btm573

Lavrov, D. V., Adamski, M., Chevaldonné, P., and Adamska, M. (2016). Extensive mitochondrial mRNA editing and unusual mitochondrial genome organization in calcaronean sponges. *Curr. Biol.* 26, 86–92. doi: 10.1016/j.cub.2015.11.043

Lendenfeld, R. (1915). The sponges. 3. Hexactinellida. *Memoirs Mus. Comp. Zoology Harv. Coll.* 42 (2), 1–396.

Letunic, I., and Bork, P. (2021). Interactive tree of life (iTOL) v5: an online tool for phylogenetic tree display and annotation. *Nucl. Acids Res.* 49, W293–W296. doi: 10.1093/nar/gkab301

Lévi, C. (1964). Spongiaires des zones bathyale, abyssale et hadale. *Galathea Rep. Sci. Result. Dan. Deep-Sea Exped. Round World 1950-52* 7, 63–112.

Librado, P., and Rozas, J. (2009). DnaSP v5: A software for comprehensive analysis of DNA polymorphism data. *Bioinformatics* 25, 1451–1452. doi: 10.1093/bioinformatics/btp187

Nguyen, L. T., Schmidt, H. A., von Haeseler, A., and Minh, B. Q. (2015). IQ-TREE: a fast and effective stochastic algorithm for estimating maximum-likelihood phylogenies. *Mol. Biol. Evol.* 32, 268–274. doi: 10.1093/molbev/msu300

Perna, N. T., and Kocher, T. D. (1995). Patterns of nucleotide composition at fourfold degenerate sites of animal mitochondrial genomes. *J. Mol. Evol.* 41, 353–358. doi: 10.1007/BF01215182

Plese, B., Kenny, N. J., Rossi, M. E., Cardenas, P., Schuster, A., Taboada, S., et al. (2021). Mitochondrial evolution in the Demospongiae (Porifera): Phylogeny, divergence time, and genome biology. *Mol. Phylogenet. Evol.* 155, 107011. doi: 10.1016/j.ympev.2020.107011

Reiswig, H. M., Dohrmann, M., Kelly, M., Mills, S., Schupp, P. J., and Wörheide, G. (2021). Rossellid glass sponges (Porifera, Hexactinellida) from New Zealand waters, with description of one new genus and six new species. *ZooKeys* 1060, 33–84. doi: 10.3897/zookeys.1060.63307

Ronquist, F., Teslenko, M., van der Mark, P., Ayres, D. L., Darling, A., Höhna, S., et al. (2012). MrBayes 3.2: Efficient Bayesian phylogenetic inference and model choice across a large model space. *Syst. Biol.* 61 (3), 539–542. doi: 10.1093/sysbio/sys029

Schulze, F. E. (1885). "The Hexactinellida," in *Report on the scientific results of the voyage of H.M.S. 'Challenger', 1873-1876*. Eds. T. H. Tizard, H. M. Moseley, J. Y. Buchanan and J. Murray (Edinburgh: Her Majesty Stationery office), 437–451.

Schulze, F. E. (1886). *Über den Bau und das System der Hexactinelliden Phys. Abh. königl. preuß. Akad. Wiss. Berlin (Phys.-Math. Cl.)* 1, 1–97.

Schulze, F. E. (1887). Report on the Hexactinellida collected by H.M.S. 'Challenger' during the years 1873–1876. *Rep. Sci. Challenger Zoology* 21, 1–514.

Stothard, P., and Wishart, D. S. (2005). Circular genome visualization and exploration using CGView. *Bioinformatics* 21, 537–539. doi: 10.1093/bioinformatics/bti054

Tabachnick, K. R. (2002). "Family Rossellidae Schulze, 1885," in *Systema Porifera - a guide to the classification of sponges*. Eds. J. N. A. Hooper and R. W. M. V. Soest (New York, Boston, Dordrecht, London, Moscow: Kluwer Academic/Plenum Publishers), 1441–1505.

Tabachnick, K. R., and Lévi, C. (2004). "Lyssacinosida du pacifique sud-ouest (Porifera: Hexactinellida)," in *Tropical deep-Sea benthos 23*. Eds. B. A. Marshall and R. B. de Forg Mém. Mus. Natl. Hist. Nat. 191, 11–71.

Wyman, S. K., Jansen, R. K., and Boore, J. L. (2004). Automatic annotation of organellar genomes with DOGMA. *Bioinformatics* 20, 3252–3255. doi: 10.1093/bioinformatics/bth352

Yang, M., Gong, L., Sui, J., and Li, X. (2019). The complete mitochondrial genome of *Calyptogena marissinica* (Heterodonta: Veneroida: Vesicomyidae): Insight into the deep-sea adaptive evolution of vesicomyids. *PloS One* 14 (9), e0217952. doi: 10.1371/journal.pone.0217952

Zhang, D., Gao, F., Jakovli, I., Zou, H., and Wang, G. T. (2020). Phylosuite: an integrated and scalable desktop platform for streamlined molecular sequence data management and evolutionary phylogenetics studies. *Mol. Ecol. Resour.* 20 (1), 348–355. doi: 10.1111/1755-0998.13096

Zhang, B., Zhang, Y. H., Wang, X., Zhang, H. X., and Lin, Q. (2017). The mitochondrial genome of a sea anemone *Bolocera* sp. exhibits novel genetic structures potentially involved in adaptation to the seep-sea environment. *Ecol. Evol.* 7, 4951–4962. doi: 10.1002/ece3.3067